

Preparation and Characterization of Metal Carbide Nanoparticles

E. Purushotham

Department of Physics, SR Engineering college (Autonomous), Warangal-506 371, India

Abstract

Metal carbide (Fe_3C) powder has been prepared by a high energed ball mill. The repeated milling of the powder sample leads to lattice distortion which gives rise to microstrains in the lattice. These microstrains increase the contribution of static component of Debye-Waller factor. Thus both lattice strain and the observed Debye-Waller factor, which is the sum of static and thermal components, increase with grinding time. Thus, the resulting nanoparticle powders were characterized by X-ray diffraction (XRD) and Scanning Electron Microscopy (SEM) measurements. The integrated intensities have been measured with a Philips CWU 3710 X-ray powder diffractometer fitted with a scintillation counter using filtered $\text{CuK}\alpha$ radiation at room temperature and have been corrected for thermal diffuse scattering.

Keywords: Fe_3C Ball milling, XRD, SEM, lattice parameters, particle size, lattice strain, Debye-Waller factor.

1. Introduction

In recent years, the synthesis of nanoparticles is a subject of intensive research, because of their basic scientific interest as well as for the technological importance. The nanoparticles exhibit very interesting properties like electrical, optical, magnetic and chemical etc. and which could not be achieved by their bulk nanoparticles [1]. Nanomaterials may also be used in various technological applications like medical imaging, drug targeting, refrigeration system and other biological applications and catalysis [2].

Recently, chemists, physicists and materials scientists have shown great interest in the development of new methods for the synthesis of nanomaterials. These materials are important for further miniaturization of electric devices, nanofluids [3] to enhance efficiency of heat engines, as chemical catalysts [4, 5] and lasing materials [6]. Physical and chemical properties of these materials are highly size dependent. Therefore, it is important to develop novel techniques for the synthesis of nanomaterials.

Metal carbides are generally referred as refractory materials due to their high melting temperatures and high hardness, and are being used as cutting tools, wear-resistance parts and surface coating. They deform plastically in a manner similar to fcc metals and become relatively soft and ductile at high temperatures. Because of their high chemical stability, high Young's modulus at high temperatures, good thermal shock resistance and thermal conductivity, metal carbides are also being used as structural materials [7]. Usually, metal carbides are prepared by conventional ceramic route, which requires a very high temperature as well as good vacuum condition or ultra pure inert gas atmosphere. However, nanocrystalline metal carbides with homogeneous composition can be prepared at room temperature by mechanical alloying (MA) the stoichiometric mixture of elemental powders under inert atmosphere.

Mechanical alloying process is a very useful solid-state technique for fabrication of nanocrystalline structure with improved properties [8–11]. If the Fe–C system is composed of a very fine microstructure, which can be synthesized by MA, it is possible to produce an advanced material with high hardness, wear resistance, toughness and good magnetic properties.

The formation of the Fe_3C carbide and some hexagonal carbides [7,12,13], the formation of Fe_3C only [14–15] and the formation of the Fe_3C carbide [16–17]. For the mixtures with $x = 20\text{--}25\%$, in all the above cases Fe_3C phase was obtained after a long period of milling with significant amount of Fe as a un-reacted powder and in none of the cases microstructures of the ball-milled samples were characterized in terms of lattice strain imperfections related to physical properties of the prepared materials.

The objectives of the present work are (i) to produce nanocrystalline Fe_3C by high-energy ball milling of Fe and C (graphite) powders at room temperature, (ii) to calculate particle size, effect of lattice strain on the Debye-Waller factor. Ball-milled samples are related to several microstructure parameters like, change in particle size, lattice strain and the effect of lattice strain on the Debye-Waller factor. All these microstructure parameters can be estimated quantitatively by analyzing the XRD patterns of ball-milled samples employing either of the method Hall-Williamson's method. As the XRD pattern of Fe_3C phase (orthorhombic) is composed of several overlapping reflections.

TEM is one of the powerful techniques for crystallite size measurement, it has certain limitations. Since TEM images represent only a local region, many samples and images are required to provide average information for the entire sample. Not only this, the TEM sample preparation method is an involved and time consuming one. The XRD technique is free from these limitations. X-ray diffraction is, on the other hand, a simple and easier approach for determination of crystallite size of powder samples.

The Debye-Waller factor is an important lattice dynamical property. There is considerable X-ray work

on the Debye-Waller factors of Fe₃C. But it is interesting to study the effect of particle size and lattice strains on the Debye-Waller factors of these metals. Pradhan et al [18] studied the Microstructure characterization of nanocrystalline Fe₃C synthesized by high-energy ball milling. Glushenkov et al [19] showed reactive ball milling to produce nanocrystalline ZnO. Inagaki *et al* [20, 21] showed that in several non-metallic powders, the strains produced during grinding have a significant effect on the Debye-Waller factors measured from X-ray diffraction intensities. Sirdeshmukh *et al* [22] observed the effect of lattice strains on the Debye-Waller factors in semiconductor powder materials. Gopi Krishna and Sirdeshmukh [23] studied the effect of lattice strains on the Debye-Waller factor of ytterbium metal. Gopi Krishna et al [24] studied the effect of lattice strains on the Debye-Waller factor of Mg, Zn and Cd for slow grinding in an agate mortar. In the present investigation the results of a systematic study of the lattice parameters, effect of particle size and lattice strains on the Debye-Waller factors of Fe₃C metal powder is reported using ball mill. These results are being reported for the first time.

2. Experimental

Experimental profiles of un-milled and all ball-milled powders are therefore fitted with the simulated powder diffraction patterns generated considering the contribution from following three phases: (i) α -Fe (cubic, space group: Im3m, a = 0.2866 nm), (ii) graphite © (hex, a = 0.2740 nm, c = 0.6707 nm, space group: P63/mmc) and (iii) Fe₃C (orthorhombic, space group: Pnma, a = 0.5091 nm, b = 0.6743 nm, c = 0.4526 nm). Highly pure α -Fe and graphite rods obtained from the solid State Physics Laboratory, New Delhi was used. The powder samples were obtained by gently filing highly pure Fe and graphite rods with a jeweler's file and mixed in 3:1 molar ratio of Fe and C. A part of this powder was used to prepare the initial sample. The remaining powder was subjected to milling in a high-energy planetary ball mill (Model: Retsch, PM 100, Germany) for 3, 6, 9, 12 and 15 hours to produce strains and decrease the particle size in a stainless steel chamber using tungsten carbide and zirconia balls of 10 mm Φ and 3 mm Φ ball sizes respectively.

The un-milled sample (0 hours) is fitted very well with Fe but with preferred orientation of graphite particles along [0 0 2]. Graphite reflections disappear within 30 min of milling and peak-broadening of Fe reflections increases continuously with increasing milling time up to 3 h of milling. This peak-broadening is fitted by considering both the effect of small particle size and lattice strain, which are reasoned due to cold working on Fe lattice during ball milling.

X-ray diffractograms were recorded with the initial sample and with samples prepared after each spell of milling. The diffractograms were obtained with a Philips CWU 3710 X-ray powder diffractometer in the 2 θ range 20-120° using filtered CuK α at a goniometer speed of 0.5° per minute and a chart speed of 20 mm/min. The XRD patterns of Fe₃C are given in Figure 1. All measurements were made at room temperature. The observed integrated intensities have been corrected for thermal diffuse scattering using the method of Chipman and Paskin [25].

3. Method of analysis

The procedure for the determination of directional mean-square amplitudes of vibration $\langle u_{\parallel}^2 \rangle$ and $\langle u_{\perp}^2 \rangle$ from the intensity data and the estimation of associated errors is as discussed by Gopi Krishna et al [26]. The average mean square amplitude $\langle u_{av}^2 \rangle$ can be obtained from the relation,

$$\langle u_{av}^2 \rangle = 1/3 (\langle u_{\parallel}^2 \rangle + 2 \langle u_{\perp}^2 \rangle) \quad (1)$$

and the directional Debye-Waller factors B_{\perp} and B_{\parallel} were obtained from the equations

$$\left. \begin{aligned} B_{\perp} &= 8\pi^2 \langle u_{\perp}^2 \rangle \\ B_{\parallel} &= 8\pi^2 \langle u_{\parallel}^2 \rangle \end{aligned} \right\} \quad (2)$$

The mean Debye-Waller factor B is given by

$$B = (2B_{\perp} + B_{\parallel}) / 3$$

The directional Debye temperatures θ_{\perp} , θ_{\parallel} and mean Debye temperature θ_M were obtained from B_{\perp} , B_{\parallel} and B, respectively using the Debye-Waller theory [27] relation,

$$\left. \begin{aligned} B &= (6h^2 / M k_B \theta_M) W(X) \\ B_{\perp} &= (6h^2 / M k_B \theta_{\perp}) W(X) \\ B_{\parallel} &= (6h^2 / M k_B \theta_{\parallel}) W(X) \end{aligned} \right\} \quad (3)$$

where h is the Planck's constant, k_B the Boltzmann constant, M the atomic weight. The function W(X) is given by

$$W(X) = [\phi(X)/X + (1/4)] \quad (4)$$

where $X = \theta_M/T$, T is the temperature of the crystal and $\phi(X)$ is the Debye function. The values of W(X) for a wide range of X can be obtained from standard tables [28].

Lattice strain and Particle size determination

When the size of the individual crystals is less than about 100nm the term “particle size” is usually used. When the crystallites of a material are smaller than 100nm, they have too small a number of parallel diffraction planes and so they produce broadened diffraction peaks instead of a sharp peak. Lattice strain present in the sample is another cause of broadening of Bragg diffraction peaks. In addition to this, there are instrumental factors such as unresolved β_1 and β_2 peaks, imperfect focusing which lead to the line broadening. There are various methods in practice to estimate the particle size. X-ray diffraction is a simpler and easier approach for the determination of precise particle size and the lattice strain in powder samples. The principle involved in the X-ray diffraction approach is precise quantification of the broadening of the Bragg diffraction peaks. Scherrer equation, Hall-Williamson method and Warren-Averbach method are some of the techniques based on this principle. Of the above methods, Scherrer equation method for the estimation of particle size does not take into account the broadening due to lattice strain present in the sample. As such in the present investigation, the lattice strains have been estimated using Hall-Williamson method. Recently, Bharati *et al* [29] have used this method to estimate the lattice strain and particle sizes of silver nano particles and composite silver nano particles. In this method the integral breadth of the diffraction peak is determined. The integral breadth is given by the integrated intensity divided by the maximum intensity. Thus, the observed peak broadening B_o may be represented as

$$B_o = B_i + B_r \quad (5)$$

where B_o is the observed peak broadening in radians, B_i is the instrumental broadening in radians and B_r is the broadening due to the small particle size and lattice strain. The instrumental broadening has been estimated using a pure strain-free fine sodium chloride powder sample subjected to XRD under identical conditions as those for the strained metallic powders. Eq. (5) holds good if the diffraction peaks exhibit purely Cauchy profile. However, when the diffraction peaks are partly Cauchy and partly Gaussian for profiles, the following relation between B_o , B_i and B_r holds good, Bharati *et al* [29].

$$B_r = [(B_o - B_i) (B_o^2 - B_i^2)^{1/2}]^{1/2} \quad (6)$$

Now, according to Scherrer equation, the broadening due to small particle size may be expressed as

$$B_c = \frac{k\lambda}{t} \cos\theta \quad (7)$$

where B_c is the broadening solely due to small crystallite size, K a constant whose value depends on particle shape and usually taken as unity, t the crystallite size in nanometers, θ the Bragg angle and λ is the wavelength of incident X-ray beam in nanometers.

Similarly, according to Wilson [30], the broadening due to lattice strain may be expressed by the relation,

$$B_s = \varepsilon \tan\theta \quad (8)$$

where B_s is the peak broadening due to lattice strain and ε the strain distribution within the material and θ is the Bragg angle. Based on Eqs. (7) and (8) the total peak broadening B_r may be expressed as,

$$B_r = \frac{k\lambda}{t \cos\theta} + \varepsilon \tan\theta \quad (9)$$

which can be written as

$$B_r \cos\theta = \frac{k\lambda}{t} + \varepsilon \sin\theta \quad (10)$$

The plot of $B_r \cos\theta/\lambda$ versus $\sin\theta/\lambda$ is a straight line with slope equal to ε and hence the particle size ‘ t ’ can be estimated from the intercept. Typical Hall-Williamson plot between $B_r \cos\theta/\lambda$ and $\sin\theta/\lambda$ is shown in Fig. (2).

The lattice strains were determined from the plot of $B_r \cos\theta/\lambda$ against $\sin\theta/\lambda$ following standard procedures [31]. The measured half-widths were corrected for instrumental broadening with reference to a pure strain-free silicon powder. The variation of particle size with milling time is within the limits of experimental errors. This shows that while the milling is enough to create strains, it affect the particle size to a measurable extent. A typical Hall-Williamson plot is shown in Fig. 2 for Zn after milling for 125 hours.

4. Results and discussion

Fig. 1 shows the XRD patterns of the Fe_3C powder ball milled at room temperature for different durations 0, 3, 6, 9, 12 and 15 hours.

Table-1. The values of the lattice parameters, particle size, lattice strain, root mean square amplitudes of vibration, Debye-Waller factors and Debye temperatures of Fe_3C powders, ground for different durations, obtained in the present study are given in Table-1. this is similar to observations of Pradhan *et al* [18].

Fig. 2 (a-d): shows The Scan Electron Microscopy (SEM) morphology of powder particles (a) 0 hours (200nm), (b) after 3 hours (12nm), (c) after 9 hours (5 nm) and (d) after 15 hours (3 nm) of milling of Fe_3C nanoparticle powders. SEM pictures are good evident for nanocrystalline state of Fe_3C nanoparticles by showing

agglomerated spherical particles of irregular-shape particles.

Both lattice strain and Debye-Waller factor increase with milling time. This is similar to observations of Inagaki et al [20, 21], Sirdeshmukh et al [22], Gopi Krishna and Sirdeshmukh [23] and Gopi Krishna et al [24]. In the present work the Debye-Waller factor increases with milling time and lattice strain in a slightly non-linear fashion.

Thus, the Debye-Waller factor Fe_3C powder sample carries an effect due to lattice strain. While comparing the Debye-Waller factors calculated from the lattice dynamical models with experimental results Vetelino et al [32] have attributed the difference to inaccuracies in the experimental values caused by neglecting the TDS corrections. The repeated milling of the powder sample leads to lattice distortion which gives rise to microstrains in the lattice. These microstrains increase the contribution of static component of Debye-Waller factor. Thus both lattice strain and the observed Debye-Waller factor, which is the sum of static and thermal components, increase with grinding time. Thus, whenever Debye-Waller factors are determined from X-ray intensities on powder samples, it is desirable, to make an estimate of the lattice strain and if the strain is large, a suitable correction is to be made as in the present study. The Debye temperatures derived from the zero strain values of Debye-Waller factor of Fe_3C is 289K.

Glyde [33] derived the following relation between the energy of vacancy formation (E_f) and the Debye temperature (θ) of a solid. The relation is

$$E_f = A(k/h)^2 M\theta^2 a^2 \quad (11)$$

where a is the interatomic spacing, A a constant shown to be equal to 1.17×10^{-2} , M the molecular weight and h and k are the Planck's and the Boltzmann's constants, respectively. Glyde recommended the use of X-ray based values in eq. (11). The validity of eq.(11) was verified for a number of fcc,bcc and hcp metals [34]. Therefore, the X-ray Debye temperatures obtained in the present work have been used to study the variation of vacancy formation energy as a function of lattice strain in Zn. The values of vacancy formation energies are also included in Table-1.

5 CONCLUSION

Fe_3C powder was strained by milling for 10 hours. From a study of X-ray diffractograms recorded at different stages of milling, it is observed that milling for 10 hours has systematic effect on the particle size. However, the milling produces lattice strain and also enhances the effective Debye-Waller factor. By an extrapolation of the plot between the Debye-Waller factor and the lattice strain, the zero strain Debye-Waller factors are obtained for Fe_3C . The variation of energy of vacancy formation as a function of lattice strain has been studied.

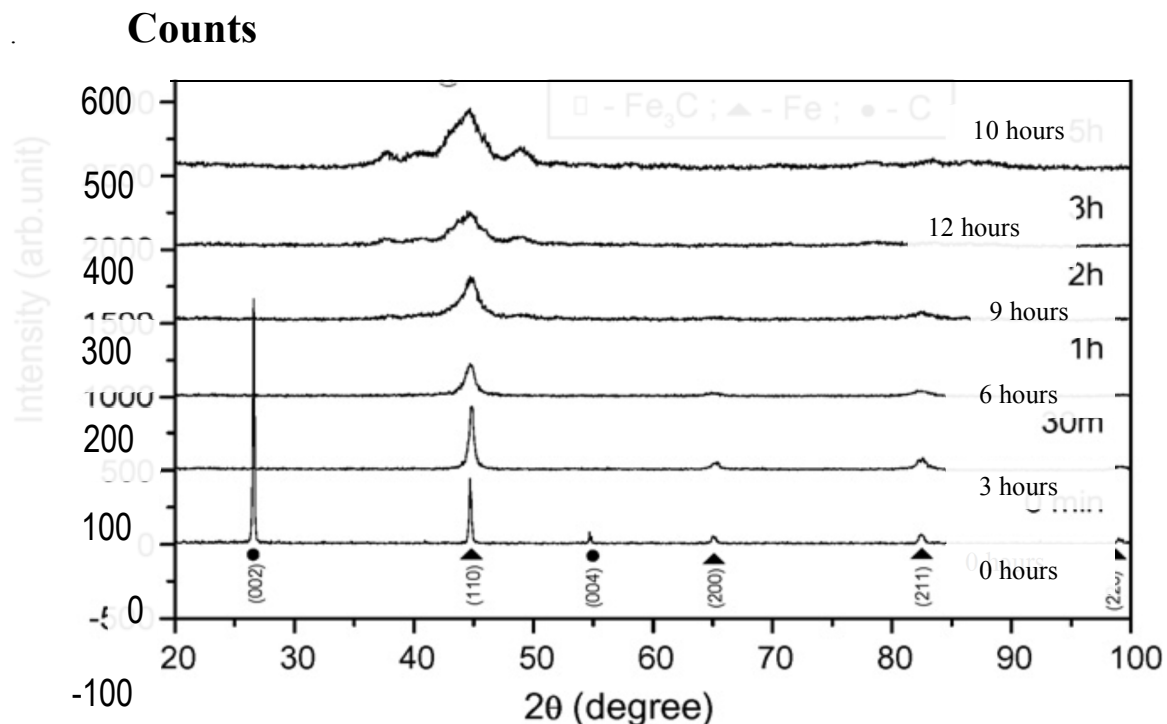


Fig. 1. X-ray powder diffraction patterns of Fe_3C

Table (1). Values of particle size (t), lattice strain (ϵ), mean Debye-Waller factor (B), root mean square amplitudes of vibration $\langle u \rangle$, mean Debye temperature (θ_M) of strained nznO Fe_3C powder.

Metal	Milling time (hrs)	$\epsilon \times 10^3$	t(nm)	a (nm)	b (nm)	c (nm)	$\langle u \rangle$,	B(\AA^2)	$\theta_M(K)$
Fe_3C	0	1.1526	198.67	0.5091	0.6743	0.4526	0.0063	0.30	274
	3	2.4128	12.12	0.5078	0.6792	0.4532	0.0076	0.46	226
	6	8.9521	4.56	0.5096	0.6784	0.4521	0.0098	0.93	165
	9	9.0434	4.49	0.5077	0.6794	0.4521	0.0147	1.05	152
	12	11.7536	4.49	0.5076	0.6795	0.4521	0.0241	1.22	129
	15	16.6233	3.36	0.5060	0.6765	0.4515	0.0283	1.69	120

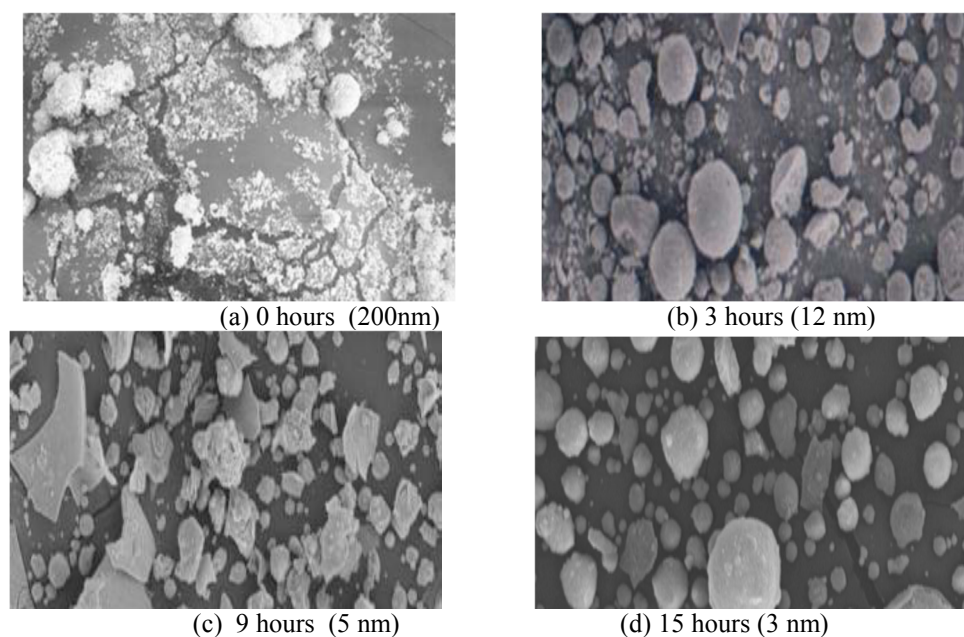


Figure 2: (a-d) The Scan Electron Microscopy (SEM) morphology of powder particles of milling of Fe_3C nanoparticle powders.

References

- [1] V L. Colvin, M.C. Schlamp and A. P. Alivisatos Nature, 370 (1994) 354.
- [2] V. Kesavan, S.P.Sivanand, S.Chandrasekaran, Y. Kolytyn and A.Gedanken Angrew. Chem. Int. Ed., 38 (1999) 3521.
- [3] J.P Abid, H.H. Girault, and P.F.Brevet, Chem. Commun. (2001) 829.
- [4] Q.Darugar, W. Qian and M.A.El-Sayed, J. Phy. Chem. B110 (2006) 143.
- [5] J.A.Eastman, S.U.S. Cnoi, and S. Li, W. Yu and L.J. Thompson, Appl. Phy Lett. 78 (2001) 718.
- [6] H. Fujiwara, S. Yanagida, and P.V. Kamat, J. Phy. Chem. B103 (1999) 2589.
- [7] G. Le Caer, P. Matteazzi, Hyperfine Interact. 66 (1991) 309.
- [8] T. Tanaka, K.N. Ishihara, P.H. Shingu, Met. Trans. 23A (1992) 2431.
- [9] A. Calka, Key Eng. 81–83 (1993) 17.
- [10] C. Suryanarayana, Prog. Mater. Sci. 46 (2001) 1.
- [11] M.H. Enayati, M. Seyed- Salehi, A. Sonboli, J. Mater. Sci. 42 (2007) 5911–5914.
- [12] V.M. Nadutov, V.M. Garamus, J.C. Rawers, Mater. Sci. Forum 343–346 (2000) 721.
- [13] V.A. Shabashov, A.G. Mukoscev, V.V. Sagaradze, Mater. Sci. Eng. A 307 (2001)91.
- [14] G.Le. Caer, E. Bauer-Grosse, A. Pianelli, E. Bouzy, P. Matteazzi, J. Mater. Sci. 25 (1990) 4726.
- [15] G.Le. Caer, P. Matteazzi, E. Bauer-Grosse, B. Pultz, A. Pianelli, Colloque de Phys. Colloque 51 (Suppl. C4) (1990) c4–c151.
- [16] K. Tokumitsu, Mater. Sci. Forum 235–238 (1997) 127.
- [17] K. Tokumitsu, M.U. Memoto, Mater. Sci. Forum 360–362 (2001) 183.

- [18] S.K. Pradhan and B. J. of Alloys and Comp. 477,127-132(2009).
- [19] A.M. Glushenkov, H.Z. Zhang and Y. Chen., Mater. Lett. 62 4047-4049 (2008).
- [20] M.Inagaki, H. Furuhashi, T.Ozeki et al., J Mater Sci.6,1520 (1971).
- [21] M.Inagaki, H.Furuhashi, T.Ozeki & S.Naka, J.Mater, Sci.8,312 (1973).
- [22] D.B.Sirdeshmukh, K.G.Subhadra, K.A.Hussain, N.Gopi Krishna, B.Raghave-ndra Rao, Cryst.Res.Technol, 28,15 (1993)
- [23] N.Gopi Krishna and D.B.Sirdeshmukh, Indian J Pure & Appl Phys.31, 198 (1993).
- [24] N.Gopi Krishna et al, Indian J Phys. 84(7), 887 (2010).
- [25] D.R.Chipman and A.Paskin, J.Appl. Phys. 30,1938 (1959).
- [26] N.Gopi Krishna, D.B.Sirdeshmukh, B.Rama Rao, B.J.Beandry and K.A.Jr.Gsch-neidner, Indian J Pure & Appl Phys.24, 324 (1986).
- [27] R.W.James, The optical principles of the diffraction of x-rays (Bell and Sons, London, 1967).
- [28] International tables for X ray crystallography, Vol.III(Kynoch press, Birmingham) (1968).
- [29] Bharati, R., Rehani, P.B., Joshi, Kirit N., Lad and Arun Pratap, *Indian Journal of Pure and Applied Physics*, 44, (2006) 157-161.
- [30] Wilson, A.J.C., (1949). X-ray Optics (Methuen, London).
- [31] Kaelble, E.F., *Handbook of X-rays* (New York Mc Graw ill) (1967)
- [32] J.F.Vetelino, S.P.Gaur, S.S.Mitra, Phys. Rev. B5, 2360 (1972).
- [33] H.R.Glyde, J.Phys and Chem Solids (G.B), 28, 2061 (1967).
- [34] Micro-and Macro-Properties of Solids, Springer Series in Material Science, (2006).